Thin Solid Films 590 (2015) 141–147

Contents lists available at ScienceDirect

Thin Solid Films

journal homepage: www.elsevier.com/locate/tsf

Optical properties of Mn doped ZnO films and wires synthesized by thermal oxidation of ZnMn alloy

M. Sima [a,*], L. Mihut [a], E. Vasile [b], Ma. Sima [a], C. Logofatu [a]

[a] *National Institute of Materials Physics, 105bis Atomistilor Street, 077125 Magurele, Romania*
[b] *University "Politehnica"of Bucharest, Faculty of Applied Chemistry and Material Science, Department of Oxide Materials and Nanomaterials, No. 1-7 Gh. Polizu Street, 011061 Bucharest, Romania*

ARTICLE INFO

Article history:
Received 8 August 2014
Received in revised form 27 July 2015
Accepted 29 July 2015
Available online 1 August 2015

Keywords:
Electro-deposition
Zinc manganese alloys
Manganese-doped zinc oxide
Photoluminescence
Raman scattering
Thermal oxidation

ABSTRACT

Mn doped ZnO films and wires, having different manganese concentrations were synthesized by thermal oxidation of the corresponding ZnMn alloy films and wires electrodeposited on a gold substrate. Structural and optical properties were addressed with scanning electron microscopy, X-ray diffraction (XRD), Raman scattering and photoluminescence (PL). To estimate the manganese concentration in Mn doped ZnO films, X-ray photoelectron spectroscopy was used. XRD patterns indicate that the incorporation of Mn^{2+} ions into the Zn^{2+} site of ZnO lattice takes place. Quenching of the ZnO PL appears due to Mn^{2+} ions in the ZnO lattice. Moreover, a significant decrease in the green emission of ZnO is reported in the case of the Mn doped ZnO wire array with a Mn concentration of 1.45%. The wurtzite ZnO has a total of 12 phonon modes, namely, one longitudinal acoustic (LA), two transverse acoustic (TA), three longitudinal optical (LO), and six transverse optical branches. Compared to the undoped ZnO, a gradual up-shift of the Raman lines assigned to the 2LA and A_1 (LO) vibrational modes, from 482 and 567 cm^{-1} to 532 and 580 cm^{-1}, respectively, takes place for the Mn doped ZnO films having a Mn concentration between 2 and 15%. Additionally, in the case of the Mn doped ZnO films with 7 and 15% Mn concentration, Raman spectra show the appearance and increase in the relative intensity of the ZnO Raman line assigned to the TA + LO vibrational mode in the 600–750 cm^{-1} spectral range. For the Mn-doped ZnO wires, the presence of the Raman line peaking at 527 cm^{-1} confirms the insertion of Mn^{2+} ions in ZnO lattice.

1. Introduction

ZnO has a relatively large band gap (3.37 eV) and high exciton binding energy (60 meV) at room temperature which makes it an excellent host material for doping of transition metal ions [1]. Mn is an isovalent impurity for Zn, and the Mn^{2+} ionic radius (0.08 nm) is comparable to that of Zn^{2+} (0.074 nm) [2], which assures a theoretical solubility limit of 35% [3] while maintaining the wurtzite structure. Most of the studies have been focused on Mn doped ZnO magnetic and spintronic properties, due to its diluted magnetic semiconductor behavior [4]. Theoretical and experimental studies [5,6] have confirmed the existence of ferromagnetism in Mn doped ZnO explained by the exchange interactions between magnetic moments localized at the Mn sites, mediated by free charge carriers. The existence of room temperature ferromagnetism has been reported in Mn doped ZnO nanorods and films for manganese concentrations of 1.3 and 2% [7] and 2 and 4% [8], respectively. On the other hand, a secondary phase was evidenced in the X-ray diffraction (XRD) pattern when manganese concentration in ZnO matrix was higher than 3%. This suggested that for manganese concentrations higher than 3% only a part of manganese ions is incorporated in ZnO matrix [9]. However recently, a concentration of manganese as high as 8% was diluted into zinc oxide epitaxial films deposited by pulsed laser deposition [10].

Various methods have been developed for the synthesis of Mn-doped ZnO nanostructures such as solvothermal [11,12] sol–gel [13], chemical vapor deposition [7,14], hydrothermal [15,16] and electrodeposition [17,18]. Incorporation of Mn in ZnO lattice via low temperature method is still difficult because of higher bond energy for Mn–O compared to that for Zn–O. Hence more energy is required to replace Zn^{2+} by Mn^{2+} in ZnO lattice [19] compared to high temperature method, where it is easier to diffuse the Mn^{2+} from vapor into the host lattice. A high temperature method used to prepare different ZnO nanostructures is thermal oxidation of Zn films or particles. Many experiments have been performed to study the ZnO thin films fabricated by thermal oxidation of zinc metallic films [20–24]. However, no work has focused on studying the oxidized films and wires prepared by thermal oxidation of ZnMn alloys. In a previous work [25], we investigated the electrodeposition process of ZnMn alloy with high manganese concentrations (22 at.%) into the submicrometer pores of a polycarbonate membrane. Among the experimental techniques used to prove the incorporation of Mn^{2+} in ZnO lattice XRD, Raman scattering and photoluminescence (PL) [26,27] have been widely used. Some authors reported that the

---

[*] Corresponding author at: National Institute of Materials Physics, P.O. Box MG 7, 077125 Magurele, Romania.
E-mail address: msima@infim.ro (M. Sima).

http://dx.doi.org/10.1016/j.tsf.2015.07.072

Table 1
Chemical composition of the solutions used for electrodeposition of Zn and ZnMn alloy films and wires and manganese content of the obtained ZnMn films.

Bath	Bath composition	Mn content of ZnMn films (at.%)
1	0.2 M complex Zn(II)-EDTA, pH 5.8	–
2	0.2 M complex Zn(II)-EDTA, 40 mM $MnSO_4$, 60 mM sodium citrate, pH 5.8	2
3	0.2 M complex Zn(II)-EDTA, 60 mM $MnSO_4$, 0.12 M sodium citrate, pH 5.8	7.5
4	0.2 M complex Zn(II)-EDTA, 20 mM $MnSO_4$, 0.18 M sodium citrate, pH 5.8	15

ferromagnetism in Mn doped ZnO thin films is controlled by the concentration of oxygen vacancies [28], and the enhancement of ferromagnetism was correlated with the increase of oxygen vacancies in ZnO [29]. Other authors [30,31] suggested that the substituting of Zn by Mn in ZnO lattice and oxygen interstitial-related defects have key roles in ferromagnetic properties. To study the defect structure of various ZnO materials, PL was employed due to its sensitivity to such defects.

In this study, Mn doped ZnO films and wires have been synthesized in two steps: electrodeposition of ZnMn alloy as films and wires followed by their rapid oxidation in a thermal process. PL and Raman scattering studies were carried out in order to characterize the oxidized structures of ZnMn alloy. It was found that a ZnO matrix which incorporated manganese ions resulting from thermal treatment of ZnMn alloy films and wires. Raman and XRD measurements signalize the substitution of Mn^{2+} for Zn^{2+} ions in the ZnO host lattice. The green emission of the oxidized films which was associated with oxygen-vacancy defects diminished at larger manganese concentrations.

2. Experimental details

Zn and ZnMn films were obtained by pulsed current electrodeposition using the solutions from Table 1, prepared after a procedure previously described [32]. The same pulsed electrodeposition was used to grow ZnMn submicrometer wires into the pores of commercial polycarbonate membranes used as template.

It is known that pulsed electrodeposition can improve physical properties of the coatings [33] and favors homogeneous nanowire growth [34]. Prior to the electrodeposition, a membrane with a thickness of about 10 μm having a pore diameter of about 800 nm and a pore density of 10^8 cm^{-2} was covered by sputtering with a thin gold film. This film was thickened by electrochemical deposition of copper layers. After the electrodeposition process the polymer membrane was dissolved in dichloromethane. Electrodeposition took place in a conventional three-electrode cell configuration at room temperature. The electrochemical cell also contained a platinum foil as an auxiliary electrode and an Ag/AgCl electrode in saturated KCl as a reference electrode. The electrochemical processes were performed using an Autolab PGSTAT 30 potentiostat digitally controlled by a computer. The as-prepared Zn and ZnMn alloy films and wires were put into a muffle furnace (Nabertherm) and heated in air for a rapid oxidation process.

The morphologies of the prepared films and wires were imaged using a field emission scanning electron microscope (FESEM) QuantaInspectF (operating voltage 30 kV) equipped for chemical composition measurements with an energy-dispersive-X-ray analysis device (resolution 129 eV at MnKα) from EDAX. XRD analyses were carried out with CuKα radiation ($\lambda = 1.5406$ Å) at 45 kV and 40 mA on a Bruker D8 Advance type X-ray diffractometer, with Bragg–Brentano diffraction geometry, equipped with a copper target X-ray tube and a LynxEye one-dimensional detector. X-ray photoelectron spectroscopy (XPS) measurement was carried out on SPECS XPS spectrometer based on Phoibos 150 electron energy analyzer with non-monochromatic X-rays emitted by an anti-cathode of Mg (1253.6 eV). The electron energy analyzer was operated in constant energy mode with pass energy of 20 eV giving an energy resolution of 0.9 eV (full-width half-maximum of the Ag 3d5/2 line). The analysis chamber was maintained in ultra high vacuum conditions ($\sim 10^{-7}$ Pa). The C (1 s) line (285 eV) corresponding to the C–C bond had been used as reference

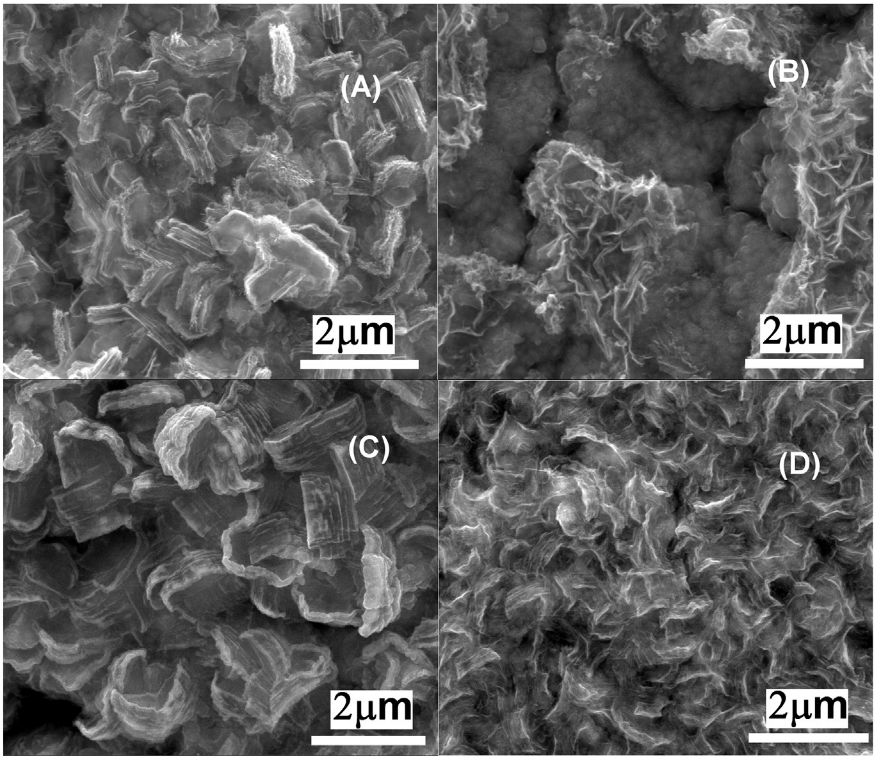

Fig. 1. FESEM images of samples obtained by thermal oxidation at 530 °C in air of the ZnMn films electrodeposited from solutions 1, 2, 3, and 4 (Table 1): (A) F1, (B) F2, (C) F3 and (D) F4.